Electronic Supplementary Material (ESI) for Nanoscale.

Ultra-bright Alkylated Graphene Quantum Dots

Lan Feng, Xing-Yan Tang, Yun-Xin Zhong, Yue-Wen Liu, Xue-Huan Song, Shun-Liu Deng,*

Su-Yuan Xie, Jia-Wei Yan, and Lan-Sun Zheng

Department of Chemistry, State Key Laboratory of Physical Chemistry of Solid Surface, College of Chemistry and Chemical Engineering, Xiamen University, Xiamen, 361005, China.

* To whom correspondences should be addressed. E-mail: sldeng@xmu.edu.cn.

1. AGQDs formed in precipitates after solvothermal reaction of PAGenes

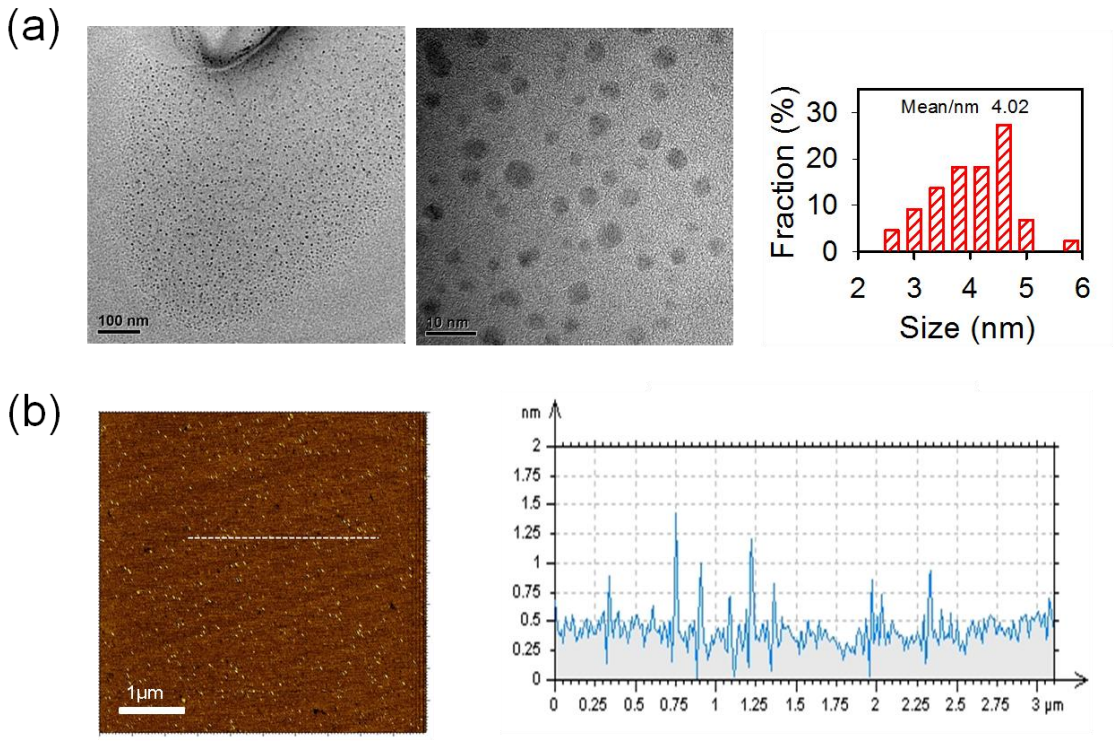

Fig. S1 AGQDs formed in precipitates after solvothermal reaction of PAGenes. (a) TEM image and size distribution of AGQDs. (b) AFM image and the corresponding height profile of a line scan.

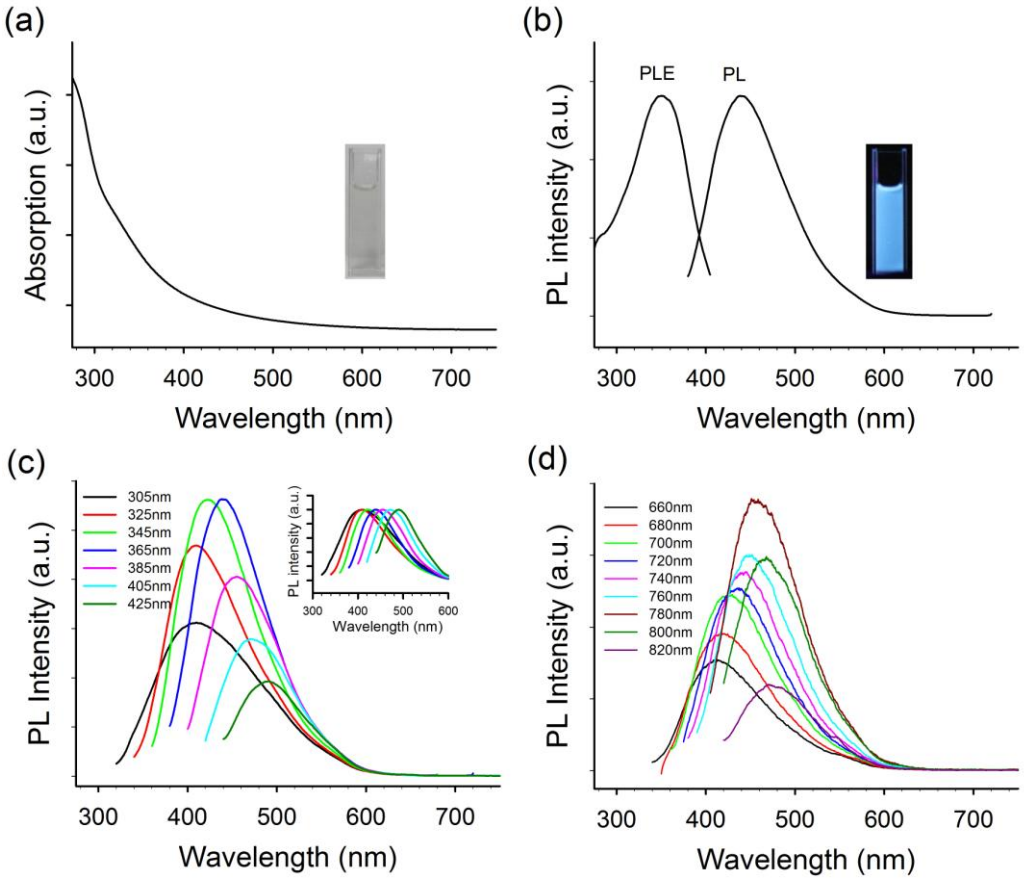

Fig. S2 The optical properties of AGQDs formed in precipitates after solvothermal reaction of PAGenes. (a) UV-Vis absorption spectrum of AGQDs in DMF dispersion (inset: photograph taken under visible light), (b) PL at 365 nm excitation and PLE with the detection wavelength of 440 nm of AGQDs (inset: photograph taken under 365 nm UV light irradiation), (c) the excitation-dependent PL behavior of AGQDs (inset: normalized to the spectral peaks), and (d) the upconversion PL properties of AGQDs.

2. **AGQDs dispersed in various solvents**

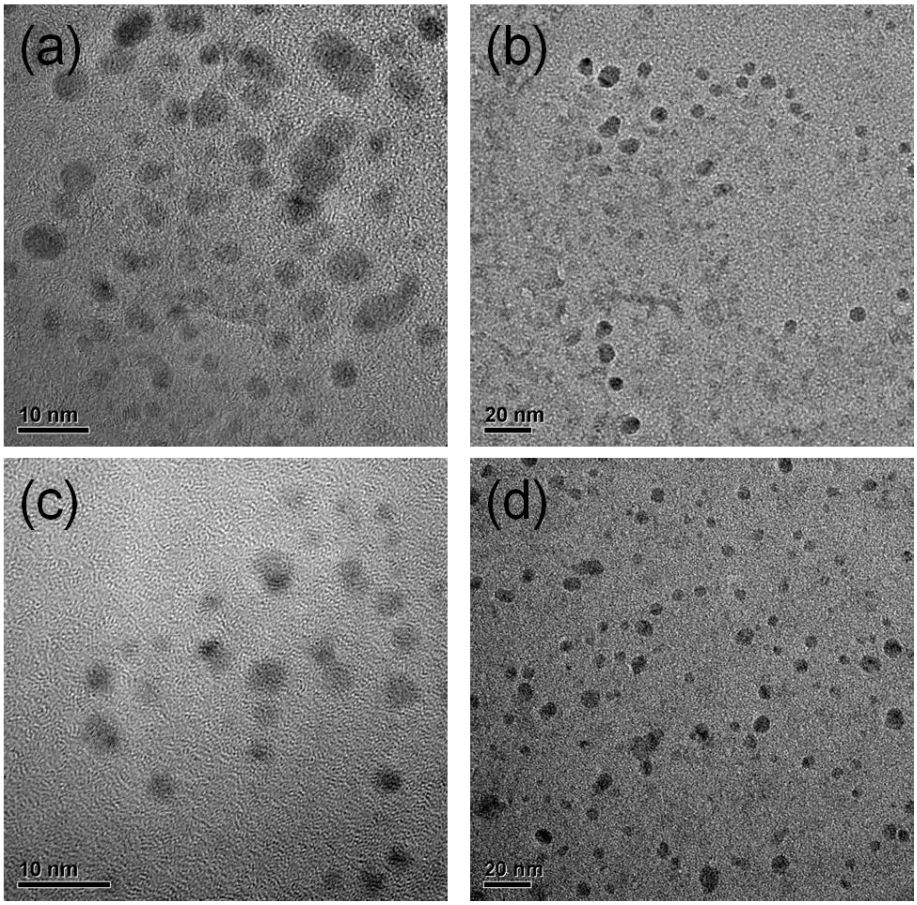

Fig. S3 TEM images of AGQDs dispersed in H_2O (a), ethanol (b), NMP (c), and cyclohexane (d), respectively.

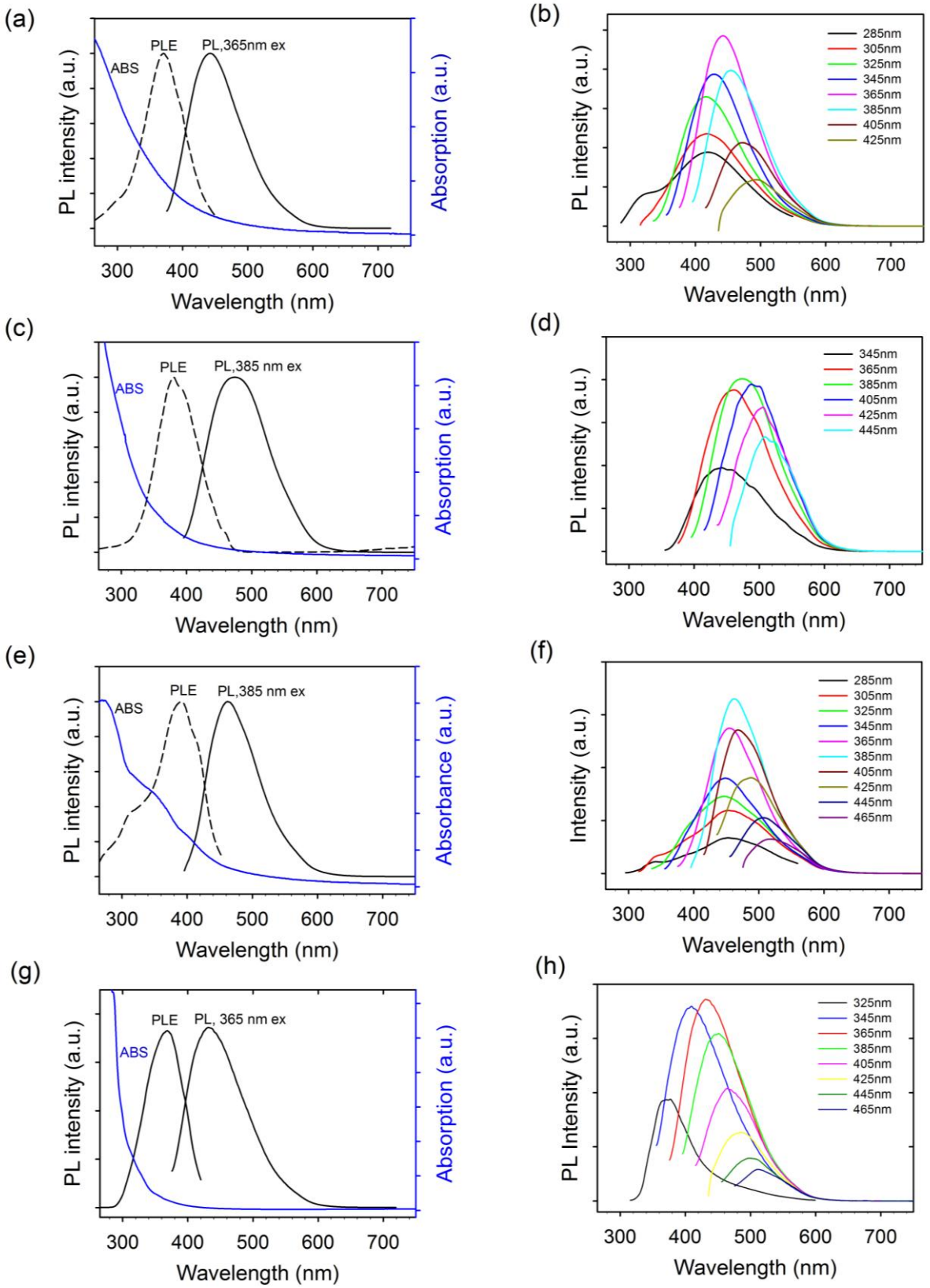

Fig. S4 Optical properties of AGQDs dispersed in H_2O (a, b), ethanol (c, d), NMP (e, f), and cyclohexane (g, h), respectively.

3. AGQDs fabricated from PAGenes-COOR by solvothermal route

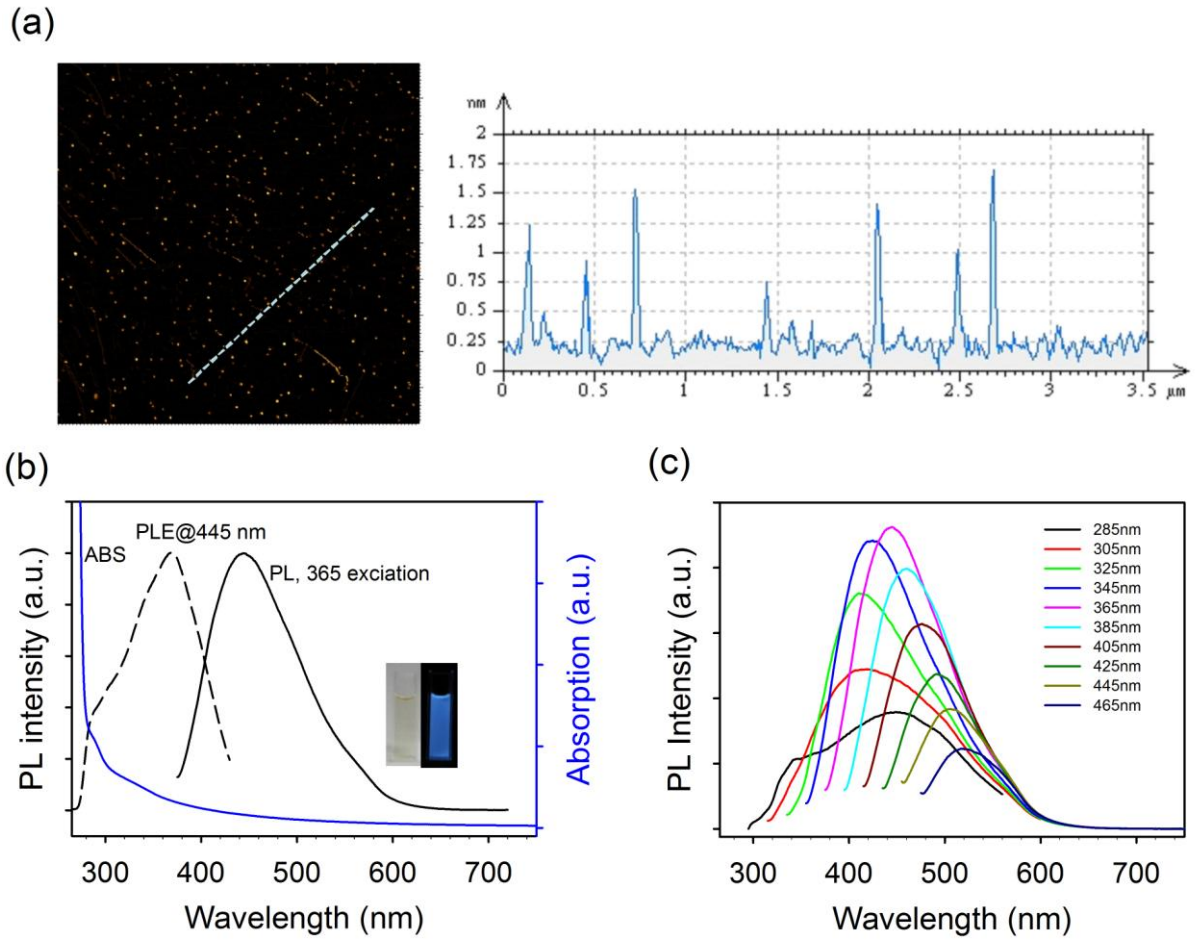

Fig. S5 AGQDs fabricated from PAGenes-COOR by solvothermal route. (a) AFM image and the corresponding height profile of a line scan, (b) UV-Vis absorption spectrum (ABS), PL spectrum at 365 nm excitation, and PLE with the detection wavelength of 445 nm of AGQDs in DMF dispersion (inset: photograph taken under visible and 365 nm UV light irradiation), (c) the excitation-dependent PL behaviors of AGQDs.

4. Quantum yield measurement of AGQDs and OAGQDs.

Using Rhodamine B in ethanol (quantum yield = 0.65) as a reference, the PL quantum yield of AGQDs (in DMF) and OAGQDs (in water) were calculated according to:

$$\phi = \phi_{st}(I_x / I_{st})(\eta_x^2 / \eta_{st}^2)(A_{st} / A_x)$$

Where ϕ is the quantum yield, I is the measured integrated emission intensity, η is the refractive index of the solvent, and A is the optical density. The subscript "*st*" refers to the reference with known quantum yield, and the subscript "*x*" refers to the sample. To minimize re-absorption

effects, absorption in the 10 mm fluorescence cuvette was kept below 0.10 at the excitation wavelength (365 nm). For AGQDs, the quantum yield was measured for three different batch samples and averaged.

Table S1 Quantum yield of AGQDs* and OAGQDs using Rhodamine B as a reference

Sample	Integrated emission intensity (I)	Abs. at 365 nm *(A)*	Refractive index of solvent (η)	Quantum Yield (ϕ)
Rhodamine B	67216.119	0.034889	1.36	0.65 (known)
AGQDs (1)	86068.6	0.04717	1.43	0.6806
AGQDs (2)	51127.982	0.031634	1.43	0.6029
AGQDs (3)	98333.108	0.055753	1.43	0.6579
OAGQDs	2865.765	0.045744	1.33	0.08558

*The average quantum yield of AGQDs is calculated to be ~ 65%.

5. Solution ^{1}H NMR spectroscopy of AGQDs

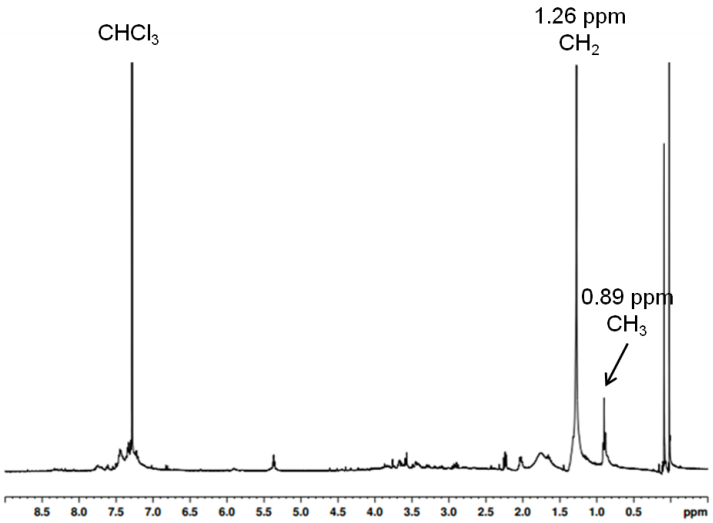

Fig. S6 ^{1}H NMR spectrum of AGQDs dispersed in $CDCl_3$. The signals for aliphatic CH_2 at 1.26 and CH_3 at 0.89 ppm clearly prove the presence of alkyl groups on AGQDs.

6. Thermogravimetric analysis (TGA) of AGQDs

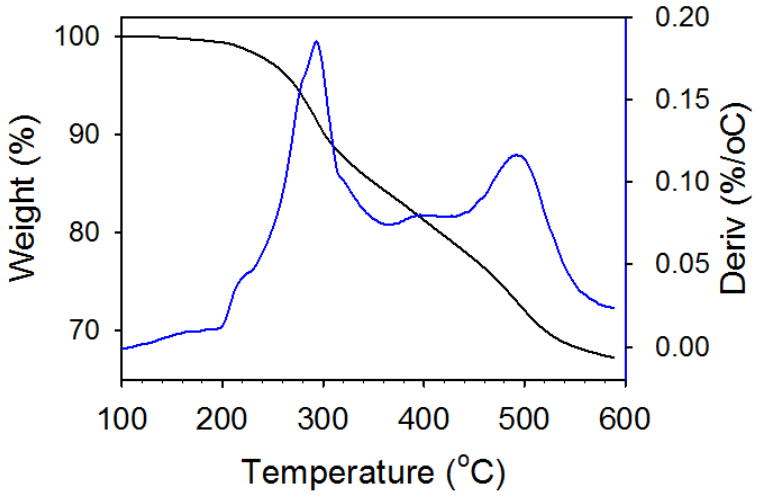

Fig. S7 TGA analysis of the synthesized AGQDs.

7. Solvothermal cutting of PAGenes versus GOs

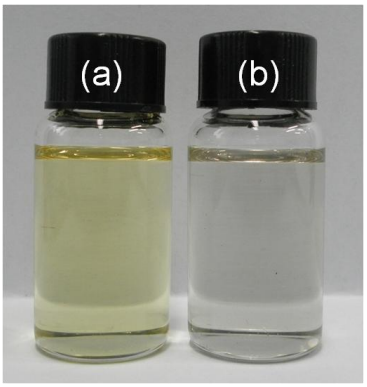

Fig. S8 Photographs of dispersions obtained from PAGenes (a) and GOs (b) by solvothermal route (200℃, 20h), followed by centrifugation at 14000 rpm for 10 min. Note that the dosage of GOs (35 mg) is ten times the weight of PAGenes (3.5 mg) in solvothermal reaction.

8. **Structural and chemical composition characterization of PAGenes**

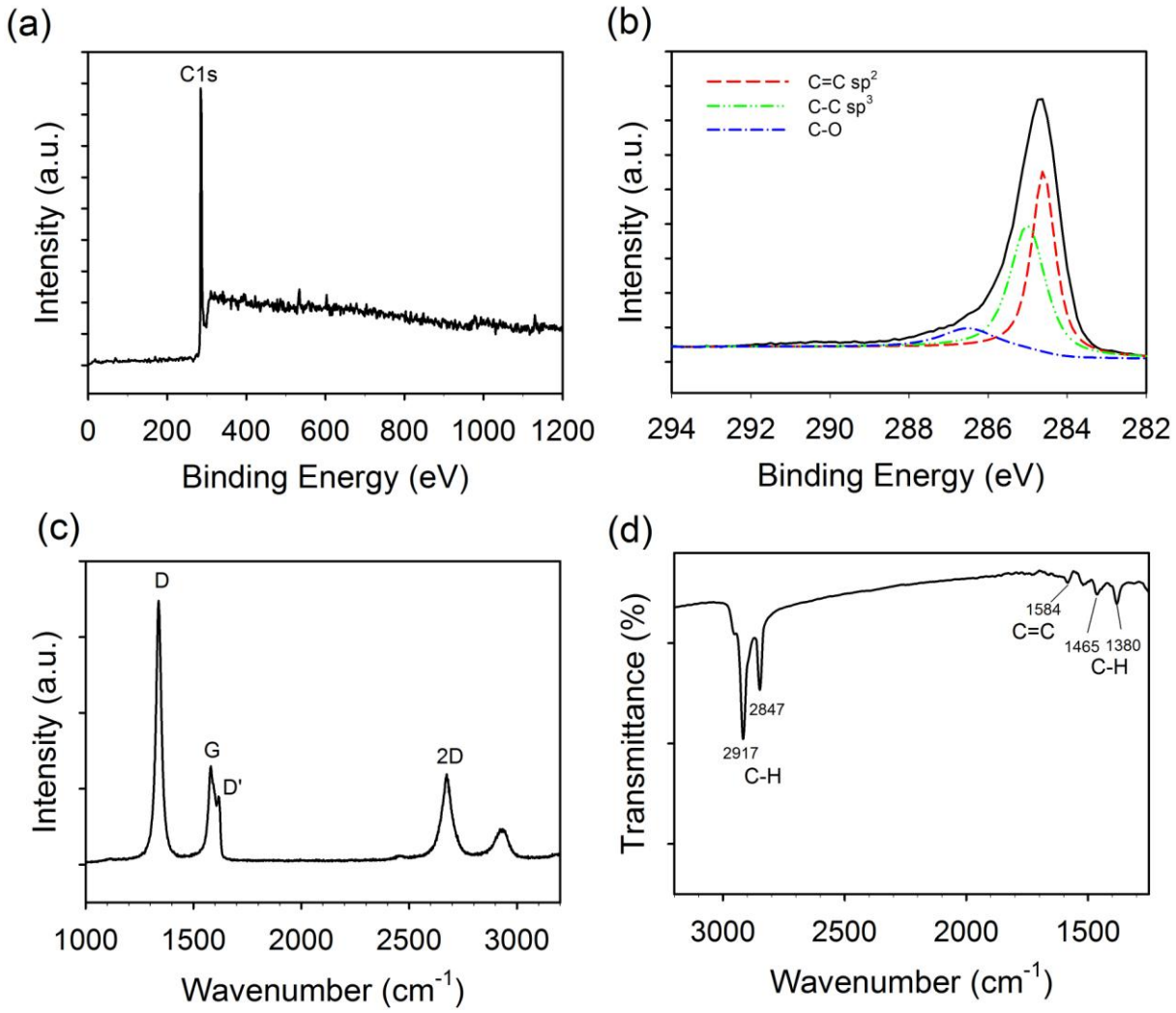

Fig. S9 Structural and chemical composition characterization of PAGenes. (a) XPS survey scan spectrum, (b) C1s high resolution XPS spectrum, (c) Raman spectrum, and (d) FTIR spectrum.

9. **Structural, chemical composition, and optical properties of OAGQDs**

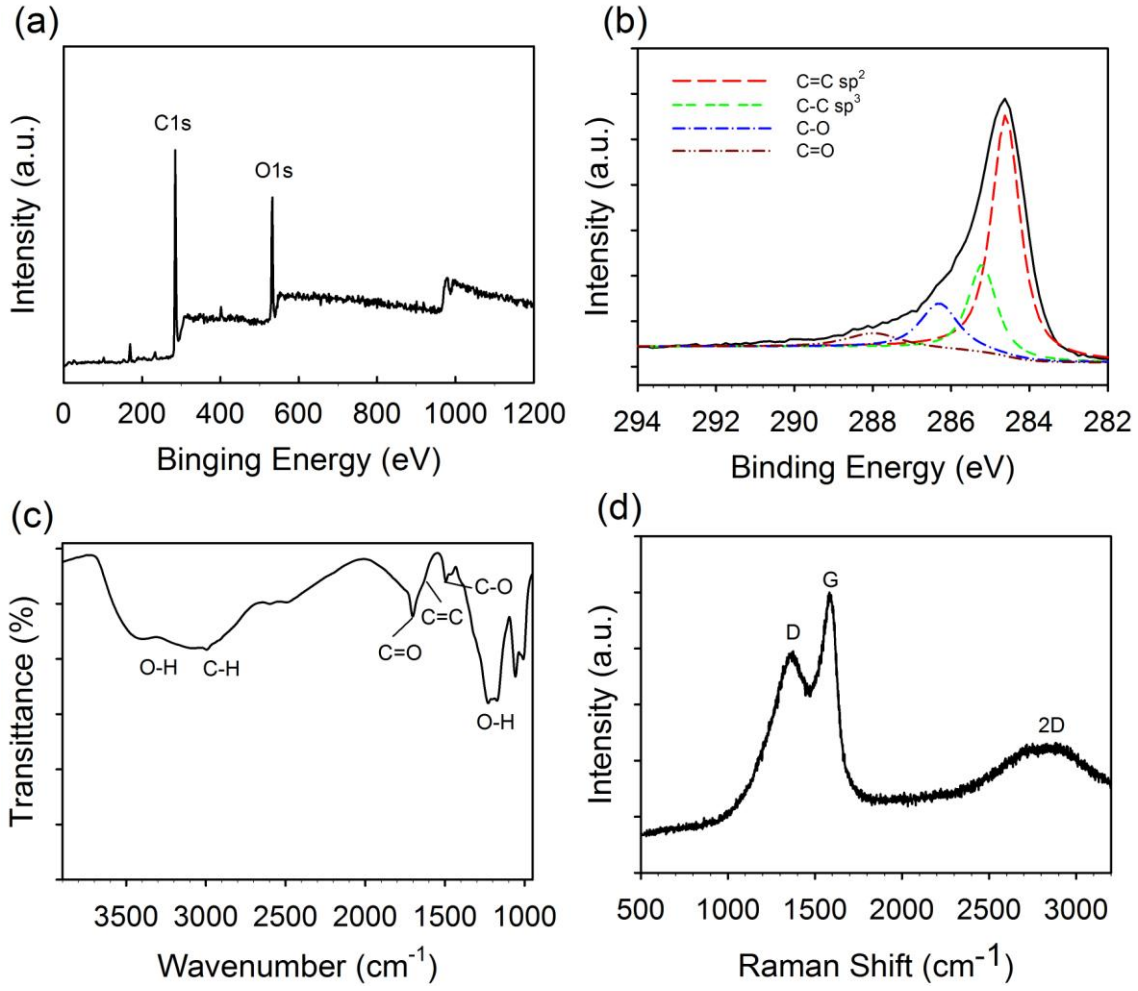

Fig. S10 Structural and chemical characterization of OAGQDs. (a) XPS survey scan spectrum, (b) C1s high resolution XPS spectrum, (c) FTIR spectrum, and (d) Raman spectrum.

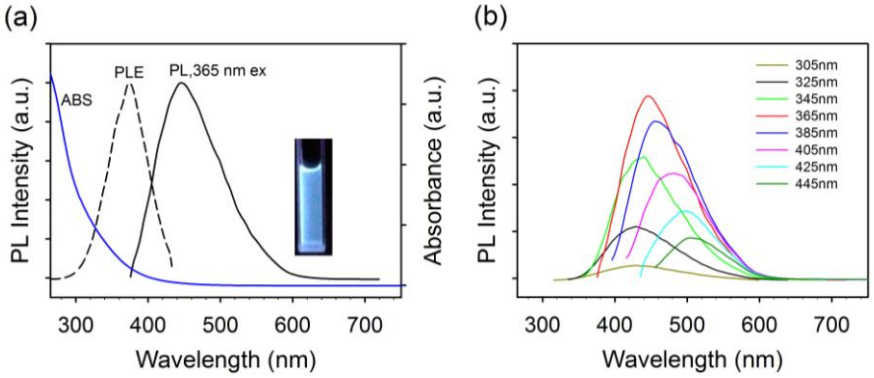

Fig. S11 Optical properties of OAGQDs. (b) UV-Vis absorption spectrum (ABS), PL spectrum at 365 nm excitation, and PLE spectrum with the detection wavelength of 445 nm of OAGQDs in water dispersion (inset: photograph taken under 365 nm UV light irradiation), (c) the excitation-dependent PL behaviors of synthesized OAGQDs.

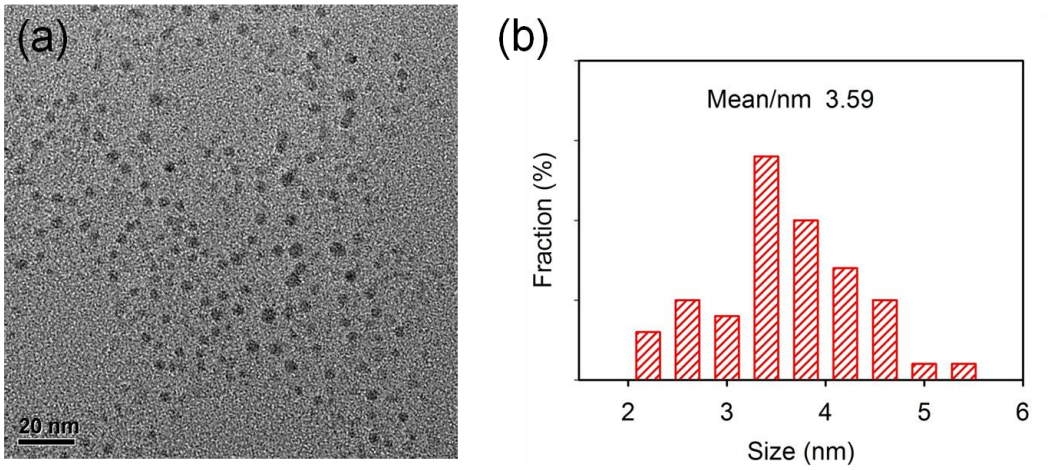

Fig. S12 TEM image (a) and size distribution (b) of OAGQDs.